

Numerical Study of Flow and Forced Heat Transfer of Robertson-Stiff Fluid Flowing Axially through Concentric Annuli

Aliakbar Heydari Gorji and Fariborz Rashidi

Department of Chemical Engineering,
The Amirkabir University of Technology (Tehran polytechnic), Hafez Ave., Tehran, Iran

Abstract

The Steady laminar axial flow of an incompressible and non-Newtonian fluid inside concentric annular spaces is analyzed. The material is supposed to behave as a generalized Newtonian liquid with Robertson-stiff stress-strain relation. Fluid flow is produced by the inner cylinder axial motion and an imposed pressure gradient in the axial direction. Both cases of positive and negative pressure gradient i.e. it assist or oppose the drag on the fluid due to the moving cylinder are studied. Four possible cases with respect to positions of the plug flow regions are considered. Heat transfer in axial flow of this viscosity function is investigated for uniform wall temperature at inner cylinder and adiabatic condition for outer cylinder. The governing momentum and energy equations have been solved iteratively by using a finite difference method. Velocity distribution, temperature profiles and Nusslet number have been obtained and compared for different values of yield stress, flow index and radius ratio in all cases mentioned above.

Keyword: Heat transfer, Axial flow, concentric annuli, non-Newtonian, Robertson-Stiff materials, Numerical simulation

Introduction

Many of the fluids used in industrial purposes are non-Newtonian and flow and heat transfer of such fluids in annuli spaces accounts for a significant part of the flow. Non-Newtonian fluids (i.e. fluid which don't obey Newtonian's law of viscosity and have an effective viscosity which is a function the shear rate) appear in many important applications and different industries including the food, sewage, pharmaceutical industries, polymer industries, cosmetics and lubricants, drilling process of oil wells and extrusion of ceramic catalyst supports. Waxy crude in the oil industry can also form non-Newtonian gels if allowed to cool below their gel-points. In all above processes and applications, the fluids, either synthetic or natural, are mixtures of different stuffs such as water, particles, oils and other long chain molecules; this combination imparts strong non-Newtonian characteristics to the resulting liquids: the viscosity function varies non-linearly with the shear rate. The fluid flows and heat-transfer behavior of non-Newtonian viscoelastic fluids has attracted special interest in recent years due to the wide application of these fluids in above processes. In these processes, heat transfer information is sometimes needed to predict temperature levels or heat transfer rate to be controlled to cause a desired rheology of the flowing material.

When one deals with a practical engineering problem consisting of a non-Newtonian fluid, it is not easy to estimate the heat transfer even in a simple geometry. The reason is that the viscosity of non-Newtonian liquids varies with both shear rate and temperature, a phenomenon which significantly influences the velocity and temperature profiles. Numerous articles about flow and heat transfer of non-Newtonian fluids can be found in the literature.

T. Shigechi et al. investigated the laminar forced convection of Newtonian fluids in concentric annuli with axially moving cores for both thermal entrance and fully developed regions, neglecting the effect of viscous dissipation on heat transfer. The moving wall of the inner cylinder deforms the fluid velocity profile near the wall region, resulting changes in velocity gradient there. Thus, viscous

dissipation may not be neglected in heat transfer involving moving boundaries. Manglik and Fang investigated numerically heat transfer to a power-law fluid through annuli. They found that the power-law index dose not change significantly the Nusselt number for concentric annular spaces [1]. Round and Yu analyzed the effects of reological parameters on velocity and pressure profiles of Herschel-bulkley fluids through concentric annuli.

Soares et al. (1999) studied the developing flow of Herschel-bulkley materials inside tubes for constant and temperature-dependent properties, taking axial diffusion into account. They observed that the temperature-dependent properties do not affect qualitatively pressure drop or the Nusselt number [3].

Soares et al. (2003) investigated the heat transfer in the entrance-region laminar axial flow of viscoplastic materials inside annulus. It is shown that the entrance length decreases as the material behavior departs from Newtonian. Also they observed that the effect of rheological parameters on the inner-wall Nusselt number is rather small [4].

Nascimento et al. analyzed the developing flow of Bingham fluids through concentric annuli. They resulted that the Nusselt number increases with the dimensionless yield stress along thermal entry region, but is nearly insensitive to it at the fully developed region.

Robertson-stiff fluids are non-Newtonian materials possessing a yield value. They are the combination of a Bingham plastic fluid and a pseudoplastic power-law fluid [5].

The constitutive equation for these fluids is as follows:

$$\tau = \left[K \frac{1}{n} |\dot{\gamma}|^{\frac{n-1}{n}} + \left(\frac{\tau_0}{|\dot{\gamma}|} \right)^{\frac{1}{n}} \right]^n \cdot \dot{\gamma} \quad \tau > \tau_0 \quad (1)$$

It may be represented in below form.

$$\tau = K[\dot{\gamma} + C]^n, \quad \tau > \tau_0 = KC^n \quad (2)$$

Where τ is shear stress, τ_0 is a yield stress, $\dot{\gamma}$ is the shear rate of strain, n is the flow behavior index, K and C are consistency and material constant respectively.

E. Santoyo et al. (2003) analyzed the Rheological behavior typified by Robertson-stiff model using the experimental rheometric data of some maize flour pastes. Figure 1 shows a schematic diagram of this model.[2]

In this paper, we are concerned with the flow and heat transfer of Robertson-stiff model in the annular space between two concentric cylinders where the inner cylinder is in axial motion and the outer cylinder is at rest. As a first approximation, rheological parameters in Equation 1 are assumed to be independent of temperature. Using a finite difference method, the momentum and energy equations have been solved numerically for a third kind of thermal boundary condition i.e. uniform temperature at inner cylinder; The outer cylinder is assumed to be perfectly insulated (adiabatic). Velocity distribution, temperature profiles and Nusslet number have been obtained and compared for different values of yield stress, flow index and radius ratio in some different cases of flow.

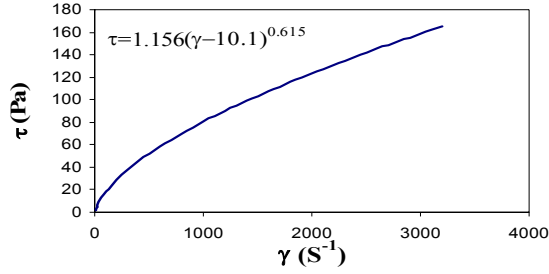


Figure 1: Rheological behavior of DPMF-13 by Robertson-stiff model [2].

Formulation and Mathematical Analysis of the Problem

A Robertson-stiff fluid confined to the space between two coaxial cylinder surfaces. The outer and inner radiuses of the concentric are R and kR , respectively. The outer cylinder is stationary while the cylinder with radius kR moves with a constant axial velocity U in the positive z direction. There is pressure gradient in the z direction, with pressure gradient being P_0 and P_L at $z = 0$ and $z = L$ respectively. The flow is supposed to be steady, laminar, incompressible and with constant pressure gradient. Local velocity is denoted by V_z and depends solely to radial distance r' .

We consider the rheological equation of state for Robertson-stiff model in cylindrical coordinate as in equation 1.

With considering the dimensionless radius and velocity, equation 1 may be simplified and rewritten in the following dimensionless form:

$$\zeta = \frac{r}{R} \quad \varphi = \frac{V_z}{U} \quad (3)$$

$$\tau_{rz} = K \left(\frac{V}{R} \right)^n \left[\left| \frac{\partial \varphi}{\partial \zeta} \right|^{\frac{n-1}{n}} + C \left(\frac{R}{V} \right) \left| \frac{\partial \varphi}{\partial \zeta} \right|^{\frac{1}{n}} \right]^n \left(- \frac{\partial \varphi}{\partial \zeta} \right) \quad (4)$$

Under the above assumptions, the momentum equations in the tangential and axial directions with negligible end effects of the cylinders in the cylindrical coordinate system with the origin at the center of the cross section of the annulus are given by

$$\frac{1}{r} \frac{\partial}{\partial r} (r \tau_{rz}) = \frac{\Delta p}{L} \quad \Delta p = p_0 - p_L \quad (5)$$

This equation after simplification to dimensionless state and integration yields the shear-stress distribution as below.

$$\tau_{rz} = \frac{\Delta PR}{2L} \left(\zeta - \frac{\lambda^2}{\zeta} \right) \quad (3)$$

and boundary conditions are

$$V_z(1) = 0 \quad , \quad V_z(k) = U > 0$$

λ^2 in equation 6 is a dimensionless constant of integration. If λ is real ($\lambda^2 > 0$), then λ corresponds mathematically to a dimensionless zero-shear radius. Equations 4 and 6 are combined and rewritten as

$$K \left(\frac{V}{R} \right)^n \left[\left| \frac{\partial \varphi}{\partial \zeta} \right|^{\frac{n-1}{n}} + C \left(\frac{R}{V} \right) \left| \frac{\partial \varphi}{\partial \zeta} \right|^{\frac{1}{n}} \right]^n \left(- \frac{\partial \varphi}{\partial \zeta} \right) = \frac{\Delta PR}{2L} \left(\zeta - \frac{\lambda^2}{\zeta} \right) \quad (7)$$

This equation will be different based on pressure or velocity gradient sign. Some of these different cases will be presented and discussed as follow.

Pressure gradient assists the drag on the fluid ($\Delta P > 0$)

λ_0, λ_i are the dimensionless boundary values of the plug flow region. $\varphi_0, \varphi_p, \varphi_i$ are the dimensionless velocity at 1) region between plug flow and inner cylinder, $k \leq \zeta < \lambda_i$, 2) plug flow region, $\lambda_i \leq \zeta \leq \lambda_0$, 3) region between outer cylinder and plug flow, $\lambda_0 < \zeta \leq 1$, respectively.

At this condition ($\Delta P > 0$) and for above regions equation 7 will be converted as below:

case I: $k \leq \zeta < \lambda_i$

$$\frac{\partial \varphi_i}{\partial \zeta} > 0 \Rightarrow -K \left(\frac{V}{R} \right)^n \left[\frac{\partial \varphi_i}{\partial \zeta} + C' \right]^n = \frac{\Delta PR}{2L} \left(\zeta - \frac{\lambda^2}{\zeta} \right)$$

$$\frac{\partial \varphi_i}{\partial \zeta} = \left[\Lambda \left(\frac{\lambda^2}{\zeta} - \zeta \right) \right]^{\frac{1}{n}} - C' \quad (8)$$

case II: $\lambda_i \leq \zeta \leq \lambda_0$

$$\frac{\partial \varphi_p}{\partial \zeta} = 0 \quad (9)$$

case III: $\lambda_0 < \zeta \leq 1$

$$\frac{\partial \varphi_0}{\partial \zeta} < 0 \Rightarrow \frac{\partial \varphi_0}{\partial \zeta} = - \left[\Lambda \left(\zeta - \frac{\lambda^2}{\zeta} \right) \right]^{\frac{1}{n}} + C' \quad (10)$$

Here, Λ and C' are denoted as

$$\Lambda = \frac{\Delta P R}{2LK} \left(\frac{R}{V} \right)^n \quad C' = C \left(\frac{R}{V} \right) \quad (11)$$

Pressure gradient opposes the drag on the fluid ($\Delta P < 0$)

Pressure gradient is negative i.e. $P_0 < P_L$ and it is caused the fluid flow in opposite direction of inner cylinder axial moving. At this condition and for three regions Equation 7 will be as

case I: $k \leq \zeta < \lambda_i$

$$\frac{\partial \varphi_i}{\partial \zeta} < 0 \Rightarrow \frac{\partial \varphi_i}{\partial \zeta} = - \left[\Lambda \left(\frac{\lambda^2}{\zeta} - \zeta \right) \right]^{\frac{1}{n}} + C' \quad (12)$$

case II: $\lambda_i \leq \zeta \leq \lambda_0$

$$\frac{\partial \varphi_p}{\partial \zeta} = 0 \quad (13)$$

case III: $\lambda_0 < \zeta \leq 1$

$$\frac{\partial \varphi_0}{\partial \zeta} > 0 \Rightarrow \frac{\partial \varphi_0}{\partial \zeta} = \left[\Lambda \left(\zeta - \frac{\lambda^2}{\zeta} \right) \right]^{\frac{1}{n}} - C' \quad (14)$$

Finally with considering of above results and equations for different cases, the following general equations are resulted.

$$\frac{\partial \varphi_i}{\partial \zeta} = \Lambda |\Lambda|^{\frac{1}{n}-1} \left(\frac{\lambda^2}{\zeta} - \zeta \right)^{\frac{1}{n}} - \frac{|\Lambda|}{\Lambda} C' \quad k \leq \zeta < \lambda_i \quad (15)$$

$$\frac{\partial \varphi_0}{\partial \zeta} = -\Lambda |\Lambda|^{\frac{1}{n}-1} \left(\zeta - \frac{\lambda^2}{\zeta} \right)^{\frac{1}{n}} + \frac{|\Lambda|}{\Lambda} C' \quad \lambda_0 < \zeta \leq 1 \quad (16)$$

Four different cases of velocity distributions between two coaxial cylinders have be studied and mathematically formulated.

Velocity profile with maximum

In this case where there is maximum in the velocity distribution between two cylindrical surfaces for determination of λ_0 we consider the following conditions.

$$\Delta P > 0, \quad \varphi_i(k) = 1, \quad \varphi_0(1) = 0 \quad \varphi_i(\lambda_i) = \varphi_0(\lambda_0)$$

$$\varphi_i = 1 + \int_k^\zeta \Lambda \left[\left(\frac{\lambda^2}{\zeta} - \zeta \right) \right]^{\frac{1}{n}} d\zeta - C'(\zeta - k) \quad (17)$$

$$-\varphi_0 = - \int_\zeta^1 \left[\Lambda \left(\zeta - \frac{\lambda^2}{\zeta} \right) \right]^{\frac{1}{n}} d\zeta + C'(1 - \zeta) \quad (18)$$

Equations 17, 18 are combined and rewritten as below:

$$\Lambda^n \left[\int_k^{\lambda_0 - \frac{\tau_0}{P}} \left(\frac{\lambda_0 \left(\lambda_0 - \frac{\tau_0}{P} \right)}{\zeta} - \zeta \right)^{\frac{1}{n}} d\zeta - \int_{\lambda_0}^1 \left(\zeta - \frac{\lambda_0 \left(\lambda_0 - \frac{\tau_0}{P} \right)}{\zeta} \right)^{\frac{1}{n}} d\zeta \right] + \quad (19)$$

$$C'(-2\lambda_0 + k + 1 + \frac{\tau_0}{P}) = -1$$

Equation 19 is used for calculating of λ_0 in case of maximum velocity profile, but it has limitation at $\lambda_i = k$. therefore $\Lambda_{critical}$ is calculated by the following equation and $\Lambda > \Lambda_{cr1}$:

$$\Lambda_{cr1} = \left[\frac{\left[1 + C' \left(k + \frac{\tau_0}{P} - 1 \right) \right]}{\int_k^{\lambda_0 - \frac{\tau_0}{P}} \left[\zeta - \frac{k \left(k + \frac{\tau_0}{P} \right)}{\zeta} \right]^{\frac{1}{n}} d\zeta} \right]^n \quad (20)$$

Velocity Profile with Plug Flow on Inner Cylinder

In this case plug flow is attached to inner cylinder and for determination of λ_0 we consider the following conditions.

$$\Delta P > 0, \quad \varphi_0(\lambda_0) = 1$$

$$\Lambda^{\frac{1}{n}} \int_{\lambda_0}^1 \left(\zeta - \frac{\lambda_0 \left(\lambda_0 - \frac{\tau_0}{P} \right)}{\zeta} \right)^{\frac{1}{n}} d\zeta + C'(\lambda_0 - 1) - 1 = 0 \quad (21)$$

Equation 21 has limitation at $\lambda_0 = k$. therefore Λ_{cr2} is calculated at $\lambda_0 = k$ by the relevant equation, in common way as previous in equation 20 and $\Lambda_{cr2} \leq \Lambda \leq \Lambda_{cr1}$.

Velocity Profile with Minimum

For this case where there is minimum in the velocity distribution, for determination of λ_0 we consider the following conditions.

$$\Delta P < 0, \quad \varphi_i(\kappa) = 1, \quad \varphi_0(1) = 0 \quad \varphi_i(\lambda_i) = \varphi_0(\lambda_0)$$

$$\Lambda^{\frac{1}{n}} \left[\int_k^{\lambda_0 - \frac{\tau_0}{P}} \left(\frac{\lambda^2}{\zeta} - \zeta \right)^{\frac{1}{n}} d\zeta - \int_{\lambda_0}^1 \left(\zeta - \frac{\lambda^2}{\zeta} \right)^{\frac{1}{n}} d\zeta \right] + \quad (22)$$

$$C'(-2\lambda_0 + k + 1 + \frac{\tau_0}{P}) = 1$$

Equation 22 has limitation at $\lambda_0 = 1$ and $\Lambda > \Lambda_{cr11}$.

Velocity Profile with Plug Flow on Outer Cylinder

Plug flow is attached to outer cylinder and for determination of λ_i , the following equation is resulted as previous.

$$\Delta p < 0, \quad \varphi_i(\lambda_i) = 0$$

$$\Lambda^{\frac{1}{n}} \int_k^{\lambda_i} \left(\frac{\lambda_i \left(\lambda_i + \frac{\tau_0}{P} \right)}{\zeta} - \zeta \right)^{\frac{1}{n}} d\zeta - C'(\lambda_i - k) = 1 \quad (23)$$

The above equation has limitation at $\lambda_i = 1$. In above four cases after calculating of λ_i or λ_0 , another parameter will be obtained by $\lambda^2 = \lambda_i \times \lambda_0$. By using of finite difference method, the momentum equations have been solved numerically at these four cases.

Temperature Profile in Concentric Annuli

The energy equation neglecting the viscous and work terms is given as

$$\rho C_p V_z = \frac{\partial T}{\partial z} = \frac{k_0}{r} \frac{\partial}{\partial r} \left(r \frac{\partial T}{\partial r} \right) \quad (24)$$

The following dimensionless variables are introduced:

$$\zeta = \frac{r}{R}, \quad z' = \frac{z}{L}, \quad \theta = \frac{T - T_w}{T_0 - T_w} \quad D_H = 2R(1-k)$$

$$P_e = \frac{\rho C_p \bar{V} D_H}{k_0} \quad F = \frac{V_z}{\bar{V}} \cdot \frac{P_e \cdot R}{2L(1-k)}$$

and finally dimensionless form of energy equation is

$$F \frac{\partial \theta}{\partial z'} = \frac{1}{\zeta} \frac{\partial}{\partial \zeta} \left(\zeta \cdot \frac{\partial \theta}{\partial \zeta} \right) \quad (25)$$

Here, \bar{V} is mean velocity and energy equation has been numerically solved, simultaneously with momentum equations, in order to obtain temperature profiles for various flow regimes.

Nu number

$$\tau_c = -\frac{dp}{dz} \cdot \frac{D_H}{4} = -\frac{\Delta p}{L} \cdot \frac{R}{2} (1-k) \quad \gamma_c = \frac{\tau_c^n - \tau_0^n}{k^n}$$

$$\eta_c = \eta(\gamma_c) = \frac{\tau_c}{\gamma_c}, \quad R_e = \frac{\rho \bar{V} D_H}{\eta_c}$$

$$Nu_z = \frac{h_z D_H}{k_0} = \frac{2(1-k) \left(\frac{\partial \theta}{\partial \zeta} \right)_{\zeta=k}}{\theta_m} \quad (26)$$

In above equations, τ_c , γ_c , η_c and θ_m are characteristic shear stress, shear rate, viscosity and bulk temperature respectively.

fRe for checking the accuracy of numerical results

The product between the friction factor and reynolds number is:

$$f Re = \frac{-16 \frac{dP}{dx} D_H}{\tau_s} \quad , \quad \tau_s = \frac{\tau_{R_0} + k \tau_{R_i}}{1+k}$$

fRe is always equal to 64 regardless the rheological behavior and the duct geometry ($fRe=64$). This matter is used during selecting stage of an appropriate mesh while obtaining numerical solution. The numerical solution was also compared with some axial flows of non-Newtonian materials. The velocity, temperature and Nu profiles obtained numerically were as it is expected theoretically and in agreement with exact / numerical solution of Herschel-Bulkley material with considering of different rheological parameters [3,4]. Our velocity trend was similar in comparison to maximum velocity of Robertson-stiff fluid in annular duct obtained by I. Machac et al. (2003) [7].

Results and Discussion

Dimensionless velocity & temperature profiles and results for some governing parameters are presented and discussed.

Velocity distribution:

Typical dimensionless axial velocity distributions for fully developed region are shown in Figures 2, 3, 4. As shown in Figure 3, lower flow indexes cause larger dimensionless velocities and wider plug flow region. Figure 4 shows the dimensionless velocity increases and plug flow region decreases with the increase in yield stress. Velocity and finally volumetric flow rate increases for larger pressure gradients and lower radius ratios, k , as expected.

Temperature profile:

Dimensionless temperature profiles and Nusselt number variation for thermal boundary condition of uniform temperature at inner moving wall are presented. For different flow regime at $\Delta P > 0$, the dimensionless temperature always decreases with axial position (Figure 5), except for $\Delta P < 0$, which increase. It is observed that the dimension velocity is almost invariant with both yield stress and flow index, Figure 6. The Nusselt variation with different rheological parameters at maximum velocity profile has been studied. It is observed that the Nu is approximately unaffected by the yield stress, but in comparison of calculated data Nu increase with τ_0 . Figure 7 shows Nusselt number increases as flow index increases. It also increases with Peclet number. Finally, it is concluded that the influence of rheological parameters on nusselt number is rather small.

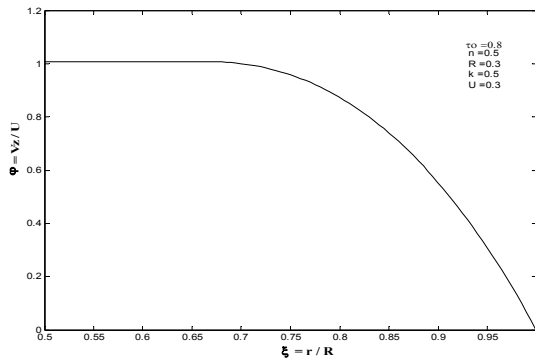


Figure 2: Velocity Distribution with plug flow on inner cylinder (Eq.21).

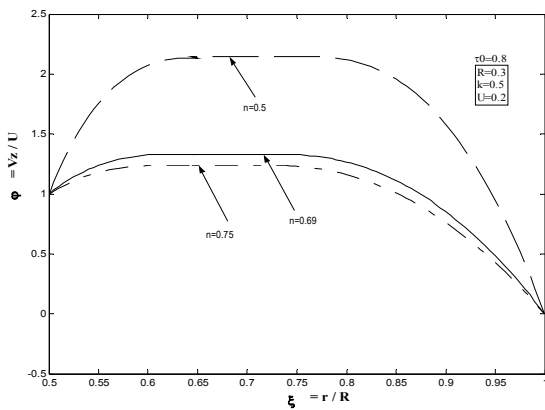


Figure 3: Velocity Distribution for different values of 'n' (Eq. 17,18,19).

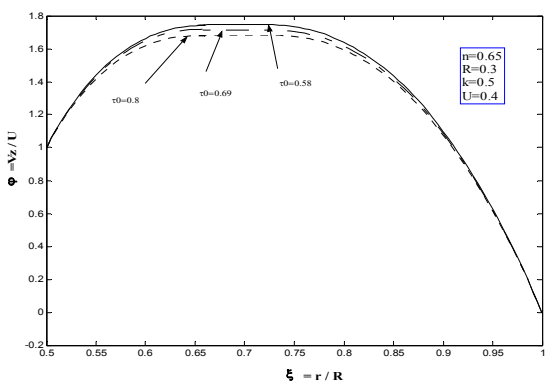


Figure 4: Velocity Distribution for different values of 'tau_0' (Eq. 17,18,19).

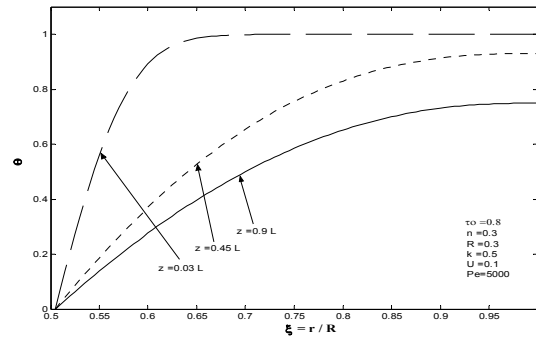


Figure 5: Temperature profile for different axial positions, for velocity distribution with maximum ($\Delta P > 0$), (Eq. 17,18,19,25).

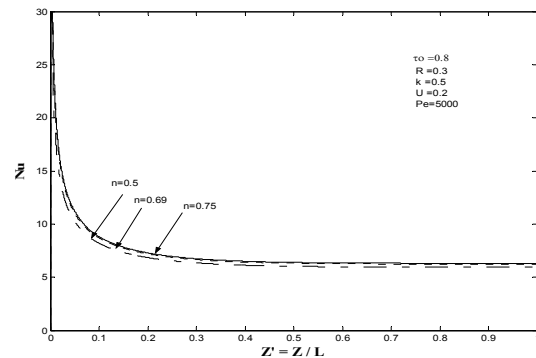


Figure 6: Temperature profile for different values of 'tau_0' (Eq. 17,18,19,25).

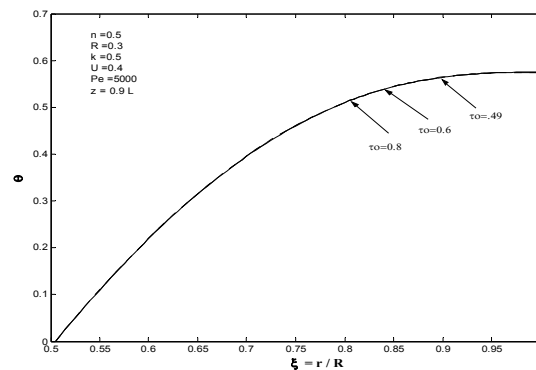


Figure 7: Nusselt number variation for different values of 'n' (Eq. 17,18,19,25,26).

References

- [1] Manglik, R., Fang, P., Thermal Processing of Various non-Newtonian Fluids in Annular Ducts, *Int. J. Heat and Mass Transfer*, **45**, 2002, 803-815
- [2] Nunez-Santiago M.C., Santoyo E., Rheological evaluation of non-Newtonian Mexican nixtamalised maize and dry processed masa flours, *Journal of Food Engineering*, **60**, 2003, 55-66.
- [3] Soares, E.J., Naccache, M.F., Souza Mendes, P.R., Heat Transfer to viscoplastic liquids flowing laminarly in entrance region of tubes, *Int. J. Heat and Fluid Flow*, **20**, 1999, 60-67.
- [4] Soares, E.J., Naccache, M.F., Souza Mendes, P.R., Heat Transfer to viscoplastic materials flowing axially through concentric annuli, *Int. J. Heat and Fluid Flow*, **24**, 2003, 762-773.
- [5] Robertson, R.E. and Stiff, H.A., An improved rheological Model for Relating Shear Stress to Shear Rate in Drilling Fluids and Cement Slurries, *Trans AIME, Soc. Pet. Eng. J.*, **261**, 1976, 31-37.
- [6] Malik, R. and Uday V. Shenoy, Generalized Annular Couette Flow of a Power-law Fluid, *Ind. Eng. Chem. Res.*, **30**, 1991, 1950-1954.
- [7] Machac I., Dolecek P., Machacova L., Poiseuille Flow of Purely Viscous Non-Newtonian Fluids through Ducts of Non-Circular Cross Section, *Chemical Engineering and Processing*, **38**, 1999, 143-148.